2018

# KINETIC MONTE CARLO SIMULATION OF BINARY ALLOYS

Timothy Craig Marshall
*Virginia Commonwealth University*

www.manaraa.com

KINETIC MONTE CARLO SIMULATION OF BINARY ALLOYS

A thesis submitted in partial fulfillment of the requirements for the degree of Master of Science at Virginia Commonwealth University.

by

TIMOTHY MARSHALL

Bachelor of Science - Longwood University - January 2013 to May 2016

Director:   Dr. Dexian Ye,

Associate Professor, Department of Physics

Virginia Commonwewalth University

Richmond, Virginia

December, 2018

**Acknowledgements**

Thank you to family, friends, and the department of physics faculty.

# TABLE OF CONTENTS

# LIST OF TABLES

# LIST OF FIGURES

## Abstract

KINETIC MONTE CARLO SIMULATION OF BINARY ALLOYS

By Timothy Marshall

A thesis submitted in partial fulfillment of the requirements for the degree of Master of Science at Virginia Commonwealth University.

Virginia Commonwealth University, 2018.

Director:   Dr. Dexian Ye,
Associate Professor, Department of Physics

There are many tools to simulate physical phenomena. Generally, the simulation technique is defined by the size of the simulation area. Two well know techniques for simulating atom dynamics are kinetic Monte Carlo (kMC) and molecular dynamics (MD). In this work we simulate physical vapor deposition of binary metallic systems using the kMC technique. A sufficient quantity of atoms are deposited so that morphological features can be observed. Where kMC has fallen short we have used MD to supplement our results.

# CHAPTER 1

## INTRODUCTION

Simulations are an important part of understanding thin films. The dynamics of these systems can not be visualized and understood without the help of theoretical tools. In addition to understanding the growth of the film, a lot of time can be saved by first running a simulation. This is due to the fact that these films have to be grown under vacuum conditions which can take days to produce. There are many simulation models available that can characterize phenomenon from the atomic to the bulk scale. Typically the spatial dimensions will determine the method of simulation. For example, finite element analysis can analyze large scale occurences such as fluid flow, while density functional theory can evolve small clusters of atoms [1,2].

Two widely used and related techniques are molecular dynamics and Monte Carlo simulations. These two techniques are useful in evaluating equilibrium driven physical systems. While Monte Carlo algorithims have broader application and faster computational time, molecular dynamics reflect the underlying physics more accurately. Discretion must be used to select the correct analytical tool not only for the purpose of computational speed but to reduce the accumulated error in thermodynamic values.

Molecular dynamics (MD) predicts the motion of an N-body system of particles by integrating Newton's equations of motion. This technique is ideal for small systems with well defined potential functions because the dynamics of the system can be calculated with a high degree of accuracy.The equilibrium state is achieved in a manner where the time dependency is preserved and the velocities of individual

1
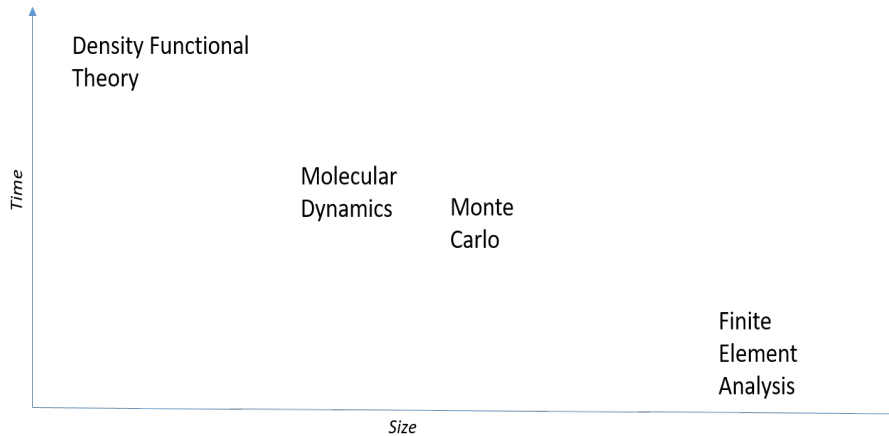
Fig. 1. Comparison of Simulations

atoms can be calculated. One of the biggest limitations of this technique is that the simulation timestep must be small enough to capture the vibrational motion of the crystal [3]. This limitation can have serious effects on the computational power required and reduces the size of crystals we can simulate. Due to the need for long simulation timesteps to create bulk crystals, roundoff errors will began to accumulate and become noticeable in the calculated thermodynamic quantities. Thus, this tool is not suitable to simulate the bulk phenomenon of crystals.

Monte Carlo simulation is a technique that employs the use of random numbers to generate events. The use of random numbers means that this tool can be used for simulations in many fields and recreate a variety of physical phenomena. We focus on a variation of MC called kinetic Monte Carlo (kMC)because it is a tool well suited to study the overall morphology of crystal growth. This method uses a list of rates to create events. For crystal growth, the rates define transitions between two sites on a lattice and are calculated using the Boltzmann factor. While in kMC there is an attempt to preserve the time dependency of the system, it is not done in a way for which atomic velocities could be calculated. Instead time serves just as a sequence of

2

events.

The experimental phenomenon we wish to recreate with our simulation is the growth of thin films. A variety of experimental techniques exist to grow films and kMC can easily be adapted to any one of them. We will simulate physical vapor deposition (PVD) because it is a consistent experimental tool that has excellent control over deposition rates and deposition angle. In the PVD setup, a crucible is heated and vapor travels in a straight line towards a substrate for it to deposit on to. Deposition rate can be controlled by adjusting the temperature and deposition angle can be adjusted by rotating the substrate with respect to the incoming vapor. This experimental tool is well known for its ability to perform glancing angle deposition (GLAD). GLAD is a variation on PVD in which atoms are deposited at oblique angles with respect to the substrate. The result is a shadowing effect that can produce helices, chevrons, and columns [4]. PVD is typically performed under a vacuum environment which can take days before gas is completely removed from the chamber. For this reason, theoretical tools are an important part in optimizing the growth conditions of deposited films.

Binary systems are an important class of thin films because of the many physical characteristics they exhibit. They can be grown under PVD depositions by alternating deposition sources or depositing both vapors concurrently. For example, in a binary system of copper and zirconium the crystal properties range from amorphous to crystalline based on the percentage of each element [5]. Under the right growth conditions this metallic glass will have improved physical characteristics such as hardness. Other binary systems such as bismuth and tellurium have thermoelectric properties that depend on the distribution of dopants. As the percentage of tellurium increases in a bismuth crystal the amount of phonon scattering increases. This improves the seeback effect by reducing thermal equilibriation while maintaining

3

electrical conductivity and thus these materials are a common choice for the design of thermoelectric devices [6]. Other important physical characteristics include the orientation of grain boundaries. Since $Bi_2Te_3$ is a topological insulator, the orientation of the grain boundaries can have interesting effects on the seeback coefficient of the material.

In this thesis we describe the details of kMC and MD. More time has been spent improving kMC so that more complex systems can be modeled. We simulate GLAD, some typical binary alloys, and grain formations within those alloys. Our results show the angles necessary to observe shadowing effects, the crystal structure of $Cu_xZr_{100-x}$, and the energy barriers necessary to observe grain boundaries.

# CHAPTER 2

# LITERATURE REVIEW

## 2.1  Monte Carlo Simulations

### 2.1.1  Markov Chains

Markov chains are a fundamental feature of any Monte Carlo algorithim so it is necessary to give at least an elementary explanation of the concept here. A Markov process is one that only depends on the intial state of the system and does not need any information about the past to make a prediction about the future [7]. For example, if given an initial state of occupied sites in a lattice the Markov process would not need to know the order that they were deposited to make a presumption about the events that would occur after. A Markov chain is then just a sequence of events that satisfy the conditon of being a Markov process. This chain can propagate in continous or discrete time but, it is mostly discrete time due to the analytical nature of computers. The easiest way to visualize a Markov chain is to imagine a sequence of coin tosses. Every event is a single coin toss that has an associated probability that is independent of the previous coin toss. It is much more common to see a Markov process in physics because it usually does not matter how a system arrived at a state. If the intial state is provided a prediction can be made about the future of the system. For example, given position and momentum of a particle, the equations of motion can be used to determine all of its future position and momentum states.

5

### 2.1.2 Importance Sampling

Consider a distribution of points that characterize a circle. If we want to render the image of the circle we could render each pixel in a screen sequentially.We could also render points along the circumference of the circle so that the visual will load faster. This illustrates the basic goal of importance sampling.The elements of a distribution are selected in such a way that defining features are accurately represented. Improving the method of sampling from a given distribution will thus improve the accuracy and efficiency of a simulation.In figure 2 we see some of the negative consequences that can occur if a poor method of sampling from a distribution is chosen.   Mathematically,

(a) An arbitrary distribution

(b) Slow sampling method

(c) Inaccurate sampling method

(d) Ideal representation
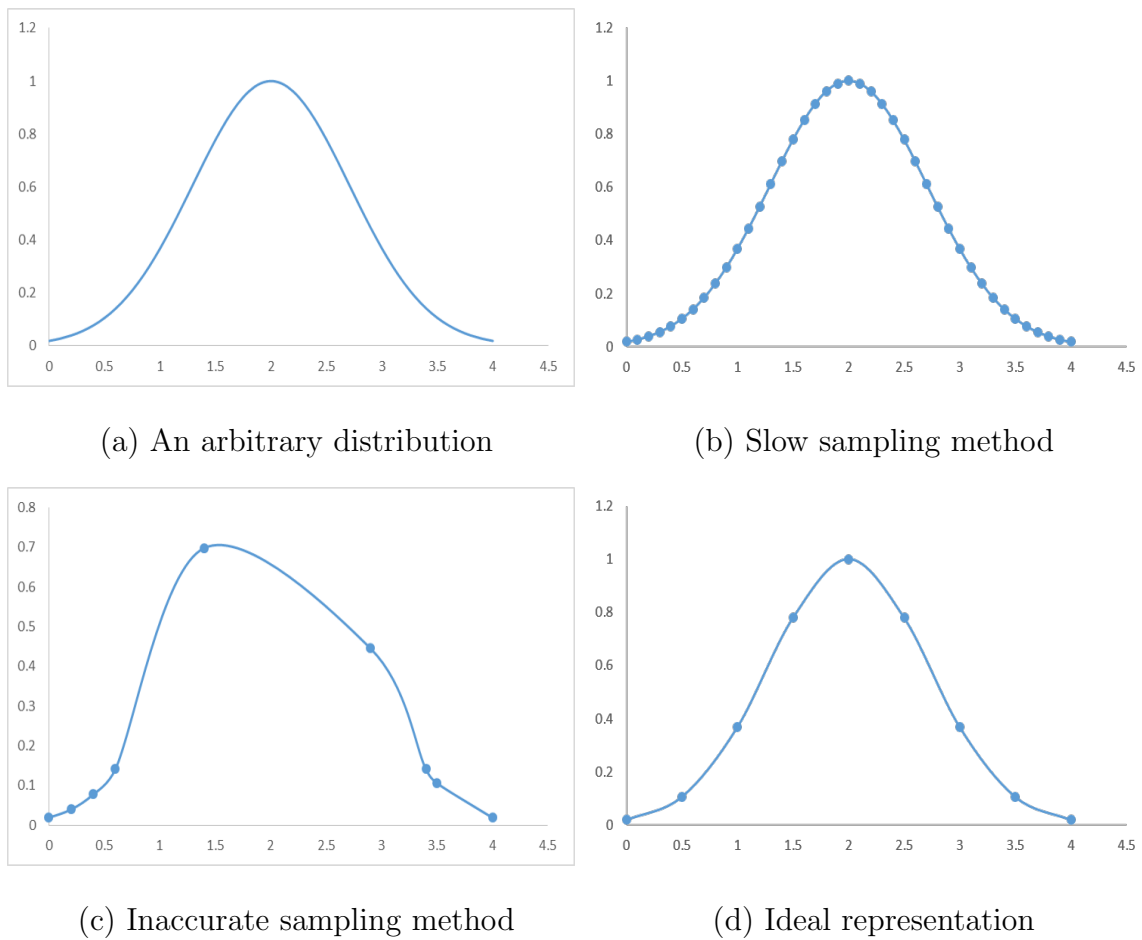
Fig. 2. Importance Sampling Example

6

importance sampling is achieved by creating an alternative distribution to supply data to a simulation other than the given distribution [7]. In the next section, we will see an example of how this is done in the kMC algorithim.

### 2.1.3  kMC Algorithim

A common type of Monte Carlo simulation is the kinetic Monte Carlo technique. The generic algorithim for this technique is defined here [3].

1. Create a list of rates for each possible event.

2. Tabulate the cumulative function.

3. Select an event to carry out.

4. Increment the simulation time

5. Update the list of rates

6. Repeat steps 3 and 4 until the desired time is reached.

More formally, if $r_j$ represents the rate of an event $j$ then the cumulative function can be expressed as.

$$R_m = \sum_{j=1}^{m} r_j \tag{2.1}$$

Where $m = 1, 2, ...M$. Events are selected by using a uniform random number to find the condition such that.

$$R_{i-1} < uR_M < R_i \tag{2.2}$$

Where $u$ is a uniform random number between zero and one. The cumulative function enables us to correctly select rates from the distribution in an appropriate manner that recognizes the need for importance sampling. In figure 3 we illustrate how an event is selected using the cumulative function. The function is bounded between 0

7
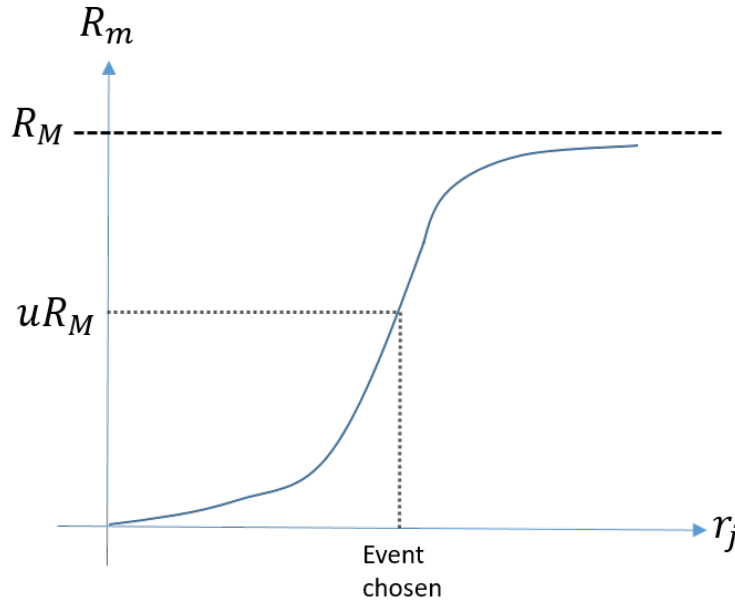
Fig. 3. Illustration showing how an event is selected using the cumulative function

and $R_M$ where M is the total numner of events. An event is picked by multiplying the total cumulative function by a uniform random number between 0 and 1 and tracing this number to the corresponding rate and event. This method of implementing importance sampling is good for evaluating ergodic Markov chains.

Timesteps are defined by the equation

$$\Delta t = -ln(u_2)/R_M \qquad (2.3)$$

Where $u_2$ represents a uniform random number that is not necessarily the same as $u$. This algorithim can be applied to any type of occurence that has an associated rate and is not limited to problems in physics. One of the most common applications of this algorithim is to use the Arhhenius equation as the rate of transitions from state to state. The transitions usually reflect an atom diffusing in a crystal, thus kMC is a good tool for analyzing problems on a lattice.

### 2.1.4   MC Variations

There are many variations on the MC algorithim. The Gillespie algorithim and the dynamic MC method are very similar with most differences between these algorithims and kMC being the field of study. One of the earliest classes of Monte Carlo algorithims was the Metropolis Monte Carlo method [8]. It is worth comparing the differences of this technique to kMC when noting the extensive usage in the literature as well as its creation setting the stage for developing kMC shortly after. The distinguishing feature of kMC is that timesteps are advanced in an appropriate manner so that the time dependence of events is preserved. In Metropolis Monte Carlo algorithims, events only have the objective to achieve equilibrium and thus no dynamics of the system are recorded [9]. One of the simplest examples of a Metropolis MC algorithim is the random walk. A random walk is a sequence of movements in which every direction has equal probabilty at every interval of movement [10]. This random walk satisfies the condition that previous movements do not affect the future probabilities of direction but it does not preserve the time dependence of the walk. The result of simulating a random walk using the Metropolis MC method is the final position of a person who walked a path while the same simulation using the kMC method would produce the path of the person over time as well as the final position.

### 2.1.5   Statistical Mechanics

Before we can apply the kMC method to simulate thin film growth we need to first review some concepts from statistical mechanics starting with the Boltzmann factor.

$$P_i = e^{-\epsilon_i/k_b t} \tag{2.4}$$

9

where t is the temperature and $k_b$ is the Boltzmann constant. This equation describes the probability that an atom has an energy eigenvalue in the ith state. If we are modeling a diffusion process then the probability that the atom can overcome some type of diffusion barrier also follows this Boltzmann factor where instead of an energy eigenvalue we have an activation energy to overcome. This activation energy can be a combination of attractive forces that keep the atom in place.

$$P = e^{-E_a/k_b t} \tag{2.5}$$

The idea of rates and probabilities are closely related but have distinct terminology that distinguish the two. When we talk about a probability we use the Boltzmann distribution which consists only of an exponential function. A rate is defined by the Arrhenius equation which differs only by a pre-exponential factor.

$$R = Z e^{-E_a/k_b t} \tag{2.6}$$

This pre-exponential factor is a constant that takes into account how many times the vibrational energy of an atom is in the correct orientation to diffuse. This pre-exponential factor has units per time thus providing us with a rate. In kMC we use rates instead of probability distributions since we want to model the dynamics of the system. Therefore, when kMC is used to model the diffusion in the system it is often said that the Arrhenius equation is used. However this is slightly deceiving because the distribution we are sampling from in the kMC algorithim does not make use of the pre-exponential factor. This constant is instead absorbed into random incrementation of time. In the literature, the Arrhenius equation and Boltzmann equation are sometimes used interchangeable for the same type of simulation.

Using the Boltzmann distribution for our kMC run is also computational convenient because this function is bounded between zero and one whereas the Arrhenius

equation has no bounds. This means that we do not have to allocate extra processor resources to scaling the associated rates to a normalized state.

This idea of a probabilty distribution is fundamental to the nature of statistical physics. The probability distribution can be used to characterize the properties of an ensemble of states and many thermodynamic quantities can be calculated by using the partition function. For a classical canonical ensemble, the partition function is defined as

$$Z = \sum e^{-\epsilon_i/k_b t} \tag{2.7}$$

In figure 4 we see an illustration of how diffusion occurs in a crystal. Atoms diffuse across an energy landscape similar to the one depicted in figure 4.a while figure 4.b shows the lattice and a nearest neighbor hop.
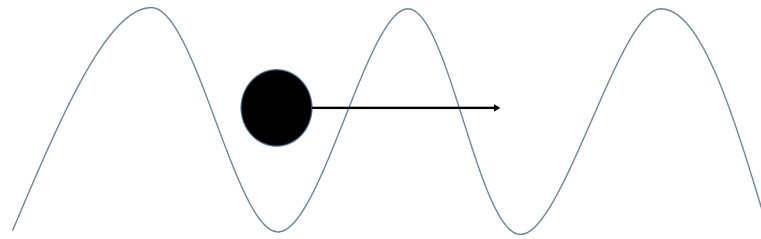
(a) Energy Landscape
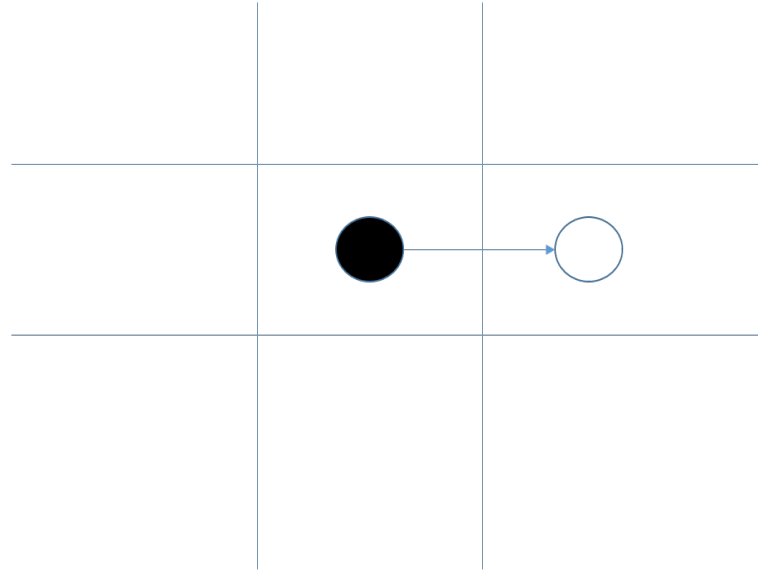


(b) Lattice Hopping

Fig. 4. An illustration of the diffusion model

## 2.2 Molecular Dynamics

### 2.2.1 Equations of Motion

From classical mechanics, the Hamiltonian of an arbitrary system is the sum of the kinetic and potential energy

$$H = T + V \tag{2.8}$$

over all the states available to the system. By applying Hamilton's equations of motion we can obtain expressions that represent the physical dynamics of an ensemble

of atoms.

$$\dot{r}_i = p_i/m_i \tag{2.9}$$

$$\dot{p}_i = f_i \tag{2.10}$$

These equations are ordinary differential equations that can be numerically integrated to obtain the motion of a system of particles. One of the most common methods to integrate these equations is by applying a Verlet integration. The Verlet algorithim is a generic scheme for calculating the previous integral and excels at maintaining conservation properties, thus this is the most widely used integration technique [11].

### 2.2.2 Potentials

The most important criteria in setting up a molecular dynamics simulation is to identify the correct potential for the type of interactions you are expecting to encounter. The potential function represents a variety of interatomic interactions that make up the attractive and repulsive forces known to the system such as Coulombic and Van Der Waals forces. Often times we can not use an exact potential as it would require very large summations, therefore it is much easier to use empirical potentials.The most common and versatile potential is the pairwise Lennard-Jones potential [12].

$$V = \epsilon[(\frac{\sigma}{r})^{12} - (\frac{\sigma}{r})^6] \tag{2.11}$$

Here, $\epsilon$ is the depth of the potential well, $r$ is the interatomic distance, and $\sigma$ is the distance for which the potential for the two atoms is zero. The Lennard Jones potental is sufficient for a variety of atoms, however a more appropriate potential for metallic systems is the Embedded Atom Model or the EAM potential [12]. The

potential is defined as

$$V = F_\alpha[\sum_{i \neq j} \rho_\beta(r_{ij})] + \frac{1}{2} \sum_{i \neq j} \phi_{\alpha\beta}(r_{ij}) \tag{2.12}$$

where $r_{ij}$ is the interatomic distance, $\phi_{\alpha\beta}$ is a pair-wise potential function,$\rho_\beta$ is the amount of electron charge density contributed to atom $i$, and $F$ represents the energy to place an atom into the electron cloud. The summation in the first term is a multibody term that includes many atoms within a certain cutoff distance. The Tersoff potential is a empirical potential that is well suited to be used for the interactions between Silicon atoms [12]. Many people have contributed and refined the Tersoff potential for Silicon so that it is accurate [13]. The potential can be expressed mathematically as

$$V_{ij} = f_c(r_{ij})[f_r(r_{ij}) + b_{ij}f_a(r_{ij})] \tag{2.13}$$

here, $f_r$ represents two body terms and $f_a$ represents three body terms. $f_c$ is simply a function to account for the cutoff distance.

These are just some of the many types of potentials that can be implemented when running a molecular dynamics simulation. In practice it is often necessary to use a hybrid style of potentials to encompass the many type of atoms that may be in the simulation. For example, Silicon is a widely studied substance with a well defined potential. Silicon wafers have very common usage in deposition, therefore it is wise to use a Tersoff potential to model the substrate and a different potential for the deposited substance.

### 2.2.3   X-Ray Diffraction

A simulation of the theoretical diffraction pattern is necessary to connect the results of simulation to experimentally obtained results. XRD can be calculated

14

alongside molecular dynamic simulations because of the emprical data included with these types of software such as the atomic scattering factor. The intensity of the x-ray diffraction spectrum is

$$I = \frac{|F| * |F|}{N} \tag{2.14}$$

$F$ represents the structure factor and is defined by

$$F(\vec{k}) = \sum_{j=1}^{N} f_j(\theta) exp(2\pi i\vec{k} \cdot \vec{r}_j) \tag{2.15}$$

k is the location of the reciprocal lattice node, $r_j$ is the position of each atom, $f_j$ are atomic scattering factors, and theta is the scattering angle of diffraction [14]. A mesh of the reciprocal lattice nodes are created for the calculation over the entire simulation domain.

15

# CHAPTER 3

## METHODOLOGY

### 3.1   kMC Energy Barriers

Just like MD requires a fair amount of consideration in choosing the potential function, so does kMC require a fair amount of consideration when determining energy values. This section is devoted to the calculation of the energy of a site and the energy barrier that limits diffusion events.

There are two different methods of limiting the diffusion of an atom by defining energy values. The first method involves determining energy values associated with each site. Diffusion would then be limited by whether the hopping event is uphill or downhill in energy. If it is downhill then the probabilty of diffusion is one. If it is an uphill energy value then the Boltzmann distribution must be used to determine the probabilty of the atom having enough energy to traverse the energy hill.

$$P = e^{\Delta E/k_b t} \tag{3.1}$$

The energy of a site is often defined as a function of the coordination number, for this method we define the Hamiltonian of a site as

$$H_i = f(n) \tag{3.2}$$

where n is the number of neighbor atoms the site is coordinated to. Mathematically we express the calculation of coordination number as

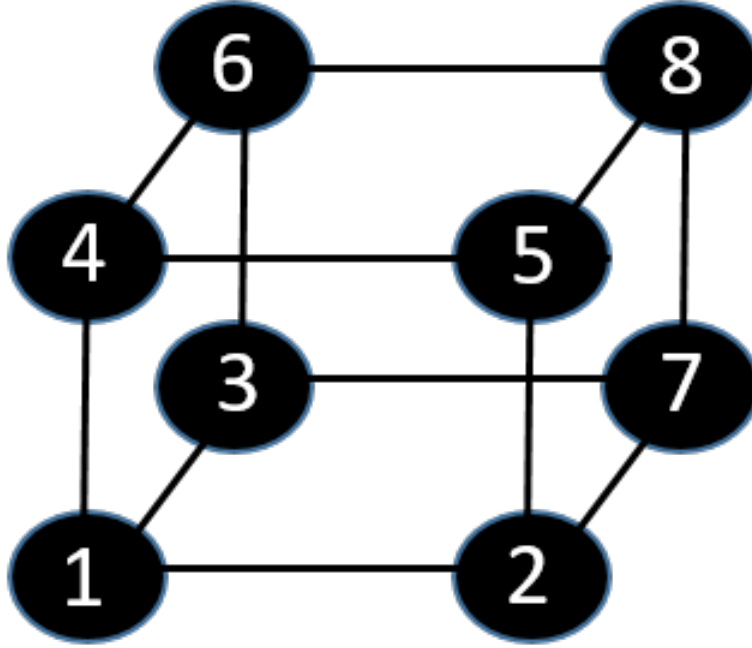$$n = \sum_j \delta_{ij} \tag{3.3}$$

16

Fig. 5. Cubic Unit Cell

where $i$ is the site in question and $j$ is a neighbor site. The delta function is one if the site is occupied. Realistically, the Hamiltonian based off this method is degenerate because it does not take into account the distance of occupied neighbor sites. For example, in figure 5, atom one has six nearest neighbors, twelve second nearest neighbor, and eight furthest neighbor.Therefore, a coordination value of six would have the highest energy when the neighbor atoms are nearest neighbors but would have a different and smaller energy value if they are not the six closest neighbors.To adequately define the energy of a site the distance between atoms should be calculated but since this requires upkeeping a floating point array and a square root function this is computationally prohibitive. Defining the energy as a linear function of co-ordination number allows us to promote the correct growth characterisitics without getting into too much detail about the bond characteristics between atoms.

17

Setting the energy of a site is one way to control the amount of diffusion that occurs in the system. This method does not discriminate based on the type of atom that is diffusing or the composition of the crystal it is diffusing in. To extend the kMC simulation technique to study structures with grain characteristics we need to create an energy barrier that accounts for these things. In this study, we propose an effective energy barrier that is a weighted average of barrier values in self diffusing crystals. Mathematically, we express this as

$$Q_{eff} = \sum_N W(n) * Q_n \tag{3.4}$$

$Q_n$ is the barrier of a self diffusing atom and $W(n)$ is a function that gives the percentage of neighbor atoms that are of type n. When we discuss our results we will use the term effective barrier to talk about a barrier that depends on the host crystal and is implemented using the previous equation. This effective barrier allows us to consider the atomic species of neighbor atoms when determining if an atom will diffuse. For example, if an occupied site had one half of its coordinated neighbor atoms of element A and another one half of element B then the effective barrier would be a half of barrier A plus a half of barrier B.

## 3.2 MD Usage

This thesis has mostly been focused on extending kMC simulations to systems with a variety of compositions. We have explored a wide variety of energy values to understand what mechanisms promote certain growth aspects however most of these values do not reflect any particular element or species. MD was used to create more realistic simulations that could be connected to experimental data. Unlike kMC, MD has much more empirical data available for specific elements.

One way which we have used MD in particular is by adjusting the position of atom

positions. Atoms from a kMC simulation are fixed on arbitrary lattice sites, but MD allows the atom positions to relax into any structure, including amorphous crystal structures. Relaxing the atom positons is necessary to calculate x-ray diffraction patterns otherwise not much information could be determined from the spectrum. To achieve relaxation of a system produced by kMC, potential functions from the previous chapter are defined and the energy is minimized. While this does not exactly preserve the time dependent evolution of our system, it is an effective way of seeing how elemental phases effect our results.

Another way which MD can be used is to calculate more realistic energy barriers. For this thesis we have simulated a variety of energy barriers to explore the effects on morphology but for a realistic simulation, MD should be used to determine an energy barrier suitable for each element.

## 3.3   Software packages

Two software programs have been used to provide the implementation of kMC and MD simulations. The first, SPPARKS, is an acronym for Stochastic Parallel PARticle Kinetic Simulator. This code was created at Sandia National Laborartory by Steve Plimpton and released under the GPL license. For kMC simulations that have a nonlinear energy value as a function of coordination number we have used the most current version of SPPARKS. For any kMC simulation that defines an effective energy barrier we have used a modified version of the SPPARKS source code. We have modified the barrier command in the SPPARKS program so that it can take multiple values. The values the barrier command take on represent the self diffusion barriers of each atom in their host crystal. Our program takes these values and implements an effective barrier as described in the section "energy barriers". More information about modifications to the code can be found in Appendix B of this thesis.

Images dumped by the SPPARKS program use the ImageMagick software suit for post processing such as converting between file formats, image resizing, and creating movies from image sequences. ImageMagick is a common tool provided with most Linux systems.

LAMMPS is a software suite created at Sandia National Laboratory as well. It is an acronym for Large-scale Atomic/Molecular Massively Parallel Simulator. This software is also released under the GPL license. We have used this software to implement MD type simulations as well as the calculation of theoretical XRD patterns. XRD simulations are provided as a user package to the software and follows an algorithim defined in the literature by Coleman. Both SPPARKS and LAMMPS have the capability of executing code in parallel using the MPI protocall. This study does not take advantage of this feature for two reasons, one being that SPPARKS does not allow deposition events for parallel runs and our simulation size was modest enough that computational tasks were not a severe hindrance. Lastly, Paraview was used to produce some of our images. The GUI interface of this program is helpful in some image processing.

# CHAPTER 4

# RESULTS AND DISCUSSION

## 4.1   Codeposited $Cu_x Zr_{100-x}$

kMC simulations were performed for various compositions of a characteristic binary metallic system. A substrate 50 atoms wide, 50 atoms long, and 4 atoms thick was initialized for atoms to deposit onto. The thermal energy ,$kt$ was specified as 0.0257, which corresponds to room temperature ( T = 25 degrees celsius). A cubic lattice with unit-less spacings of 1.0 served as a medium for atoms to propagate. The energy of the system for this set of simulations is nonlinear function of coordination number. The reason for energy being nonlinear is that a coordination value of zero was chosen to be very energetically unfavorable so that nucleation does not occur in mid air, for all other coordination values energy is linear. There is little to distinguish diffusion rate between Copper and Zirconium for this set of simulations but this is of little consequence at the moment because we do not expect large grain boundaries to form in this system. To recreate the effect of codeposition we alternate the type of atom being deposited every 100 seconds. The rate of deposition will then determine whether metal multilayers are deposited or if each element is deposited in competition with each other. Figure 6 shows films created at various deposition rates for 400 seconds total.  From figure 6 we can see that lowering the deposition rate allows us to simulate atoms being deposited at the same time. Co-deposition simulations can also be achieved by alternating the species of deposited atom at smaller time intervals. Using this method to recreate co-deposition we can simulate the distribution of a dopant in a bulk crystal. We simulated various percent compositions of an arbitrary
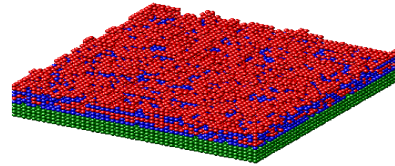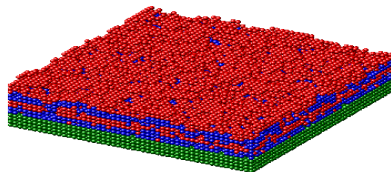
21
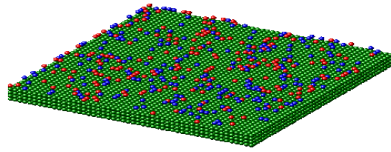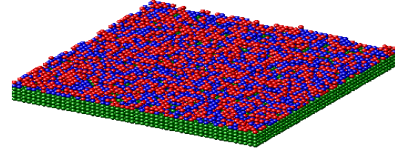
(a) 1 atom/sec

(b) 10 atom/sec
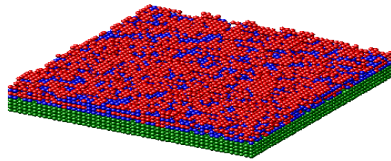
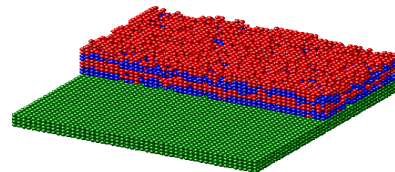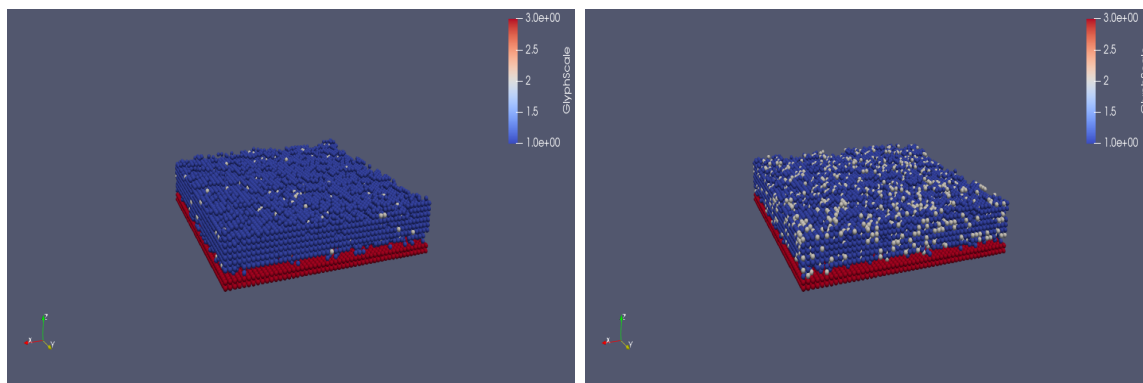(c) 25 atoms/sec

(d) 35 atoms/sec

(e) 50 atoms/sec

(f) 50 atoms/sec

Fig. 6. Deposition rate is varied while switching deposition sources every 100 seconds
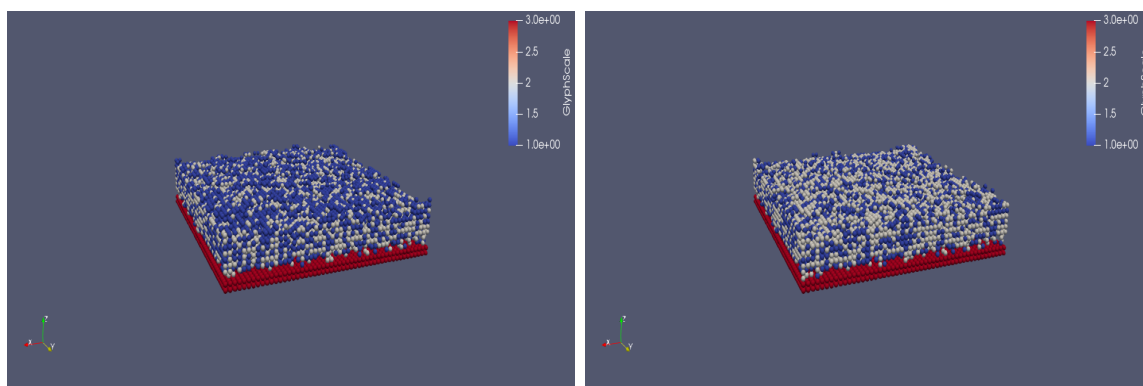
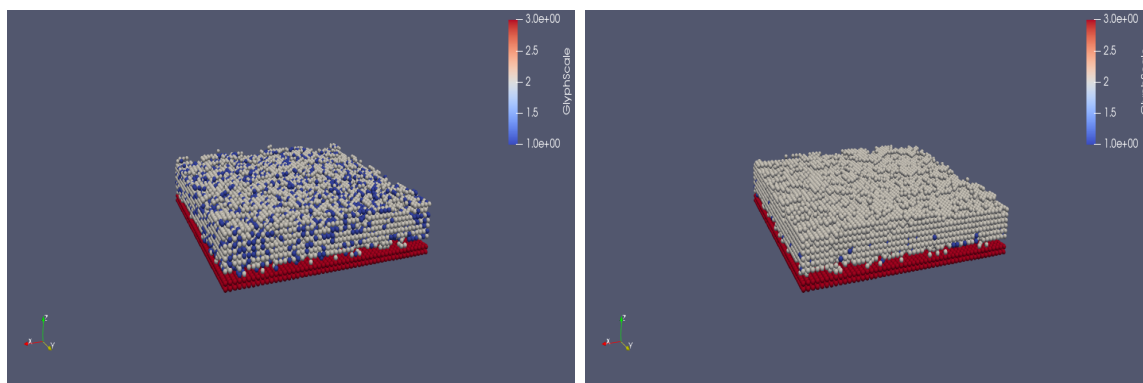binary metal. The composition of dopant ranging from 3 to 95 percent is shown below.



(a) Zr3Cu97

(b) Zr20Cu80

(c) Zr46Cu54

(d) Zr55Cu45

(e) Zr73Cu27

(f) Zr95Cu5

Fig. 7. Various compositions of deposited Zr and Cu created in SPPARKS

23

This distribution of particles can represent many binary systems but in this case we specify a system of copper and zirconium so that they can be used in MD. The atom positions are loaded in a MD type application and the lattice spacing is defined as 3 Angstroms apart. This is done to ensure that the atom positions are as close to a local minimum as possible. If the atom spacing is too compressed the atoms will have too high of a repulsive force with each other and will fly apart. If the atom positions are close enough to a local potential minimum then we can iteratively minimize the potential energy functions specified in a MD type application. This will effectively relax the the crystal structure into a more realistic and representative form. This step is necessary to gain insight into the crystallinity of our thin film because our kMC approach required atom positions to be fixed on a lattice structure that did not necessarily represent the true structure of the alloy.

By minimizing the energy of the ensemble we do not need to apply typical thermostat algorithims that adjust the velocities of the atoms to relax the system over a long period of timesteps. This greatly reduced the amount of time needed to run our simulation. Although a MD type application was used to minimize the energy, no integration of the equations of motion was applied and thus no simulation of the dynamics occured via a MD type simulation. All dynamics of the simulation were performed using the kMC approach.

To perform the potential energy minimization of the ensemble we select the following potentials, for Zr-Zr, Zr-Cu, and Cu-Cu we use the EAM potential. For the Si-Si interactions we use the Tersoff potential. For the interactions between the substrate and the deposited atoms we use the well known Lennard Jones potential. Table 2 lists the values for $\epsilon$ and $\sigma$ used for the Lennard Jones potential. Lorenz-Berthelot mixing rule was used to obtained the constant values for Zr-Si and Cu-Si interactions [5].

24

Table 1.  LJ Parameters

| Species | $\epsilon(ev)$ | $\sigma(A)$ |
|---------|--------|--------|
| Cu | 0.7382 | 2.9318 |
| Zr | 0.409 | 2.338 |
| Si | 0.0175 | 3.826 |

$$\epsilon_{ij} = (\epsilon_i \epsilon_j)^{1/2} \tag{4.1}$$

$$\sigma_{ij} = (\sigma_i + \sigma_j)/2 \tag{4.2}$$

Figures 8 and 9 show the theoretical XRD patterns of each composition $Zr_x Cu_{x-100}$ and known XRD from the literature. Table 2 provides the quantitative values of 2theta for peak positions of each composition and compares them to values provided in the literature [5]. The 2theta position of each peak agrees well with experimental values. The intensity values of the XRD pattern vary dramatically from experimental values, most likely due to the number of atoms deposited in an experiment are much larger than what our simulation is capable of. While simulation peaks tend to be much broader than experimental peaks this effect can be reduced by changing the spacing of reciprocal lattice nodes used in the XRD calculation and reducing the size of histogram bins at the cost of a relatively proportional amount of computational time. This step is likely to only smooth the curve and not account for most of the broadening. We expect a large percentage of peak broadening to be attributed to the simulation size. The potential minimization and the theoretical XRD calculation were both implemented in LAMMPS.

As the percentage of each element approaches concentrations that are equivalent

25

Table 2.   XRD Peaks

| Zr-Cu | $Zr_3Cu_{97}$ | $Zr_{20}Cu_{80}$ | $Zr_{46}Cu_{54}$ | $Zr_{55}Cu_{45}$ | $Zr_{73}Cu_{27}$ | $Zr_{95}Cu_5$ |
|---|---|---|---|---|---|---|
| Experimental | 43.2 | 41.8 | 38.7 | 37.4 | 35.9 | 34.5 |
| Simulation | 43.5 | 42.8 | 39.8 | 38.7 | 36.3 | 35.5 |

we see that the crystallinity of the structure is reduced and an amorphous structure is formed. The best condition for the formation of a metallic glass is then an equal ratio of Zr and Cu. Amorphous conditions begin for as little as 20 percent composition Zr or Cu. This makes sense if we look at the phase diagram for copper and zirconium. Figure 10 shows a change in the bonding characteristics at a little under 20 percent zirconium. From this we can see that our XRD pattern is a traversal of this phase diagram.
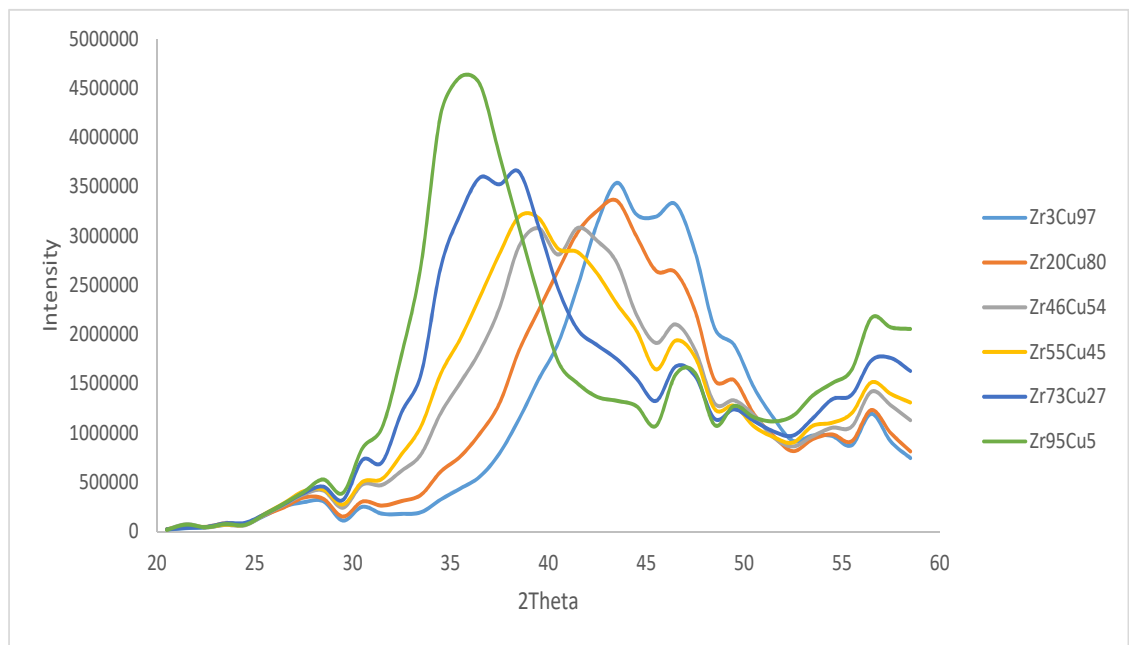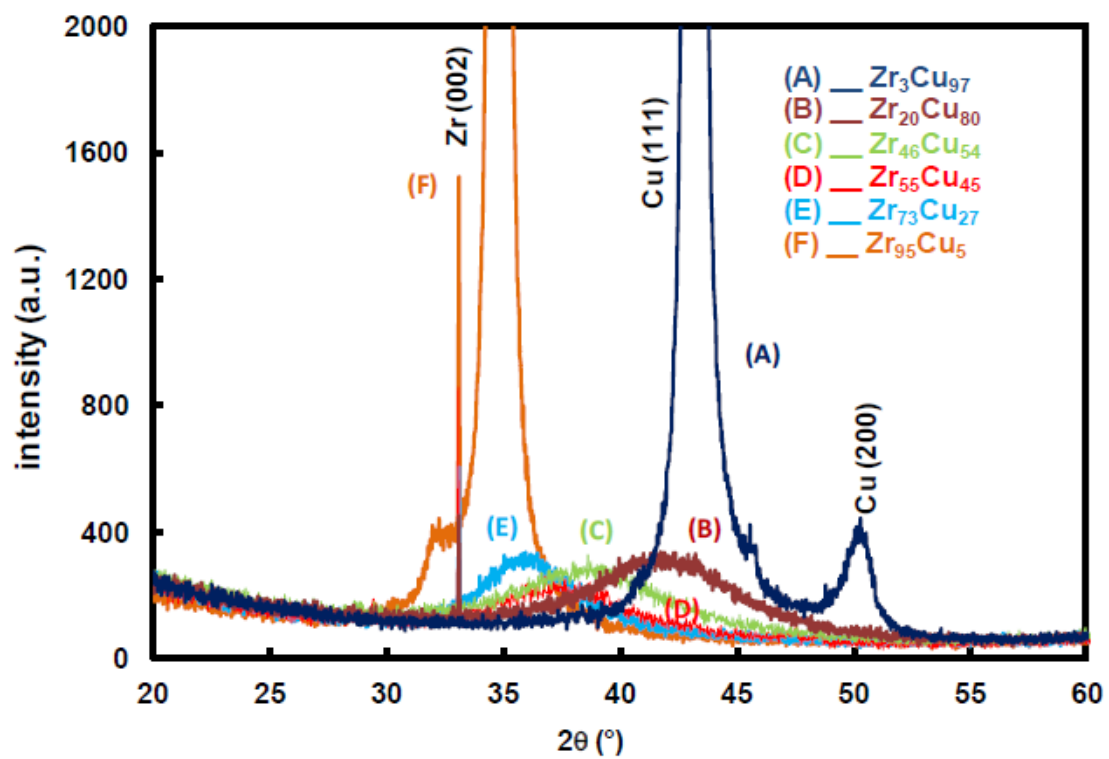
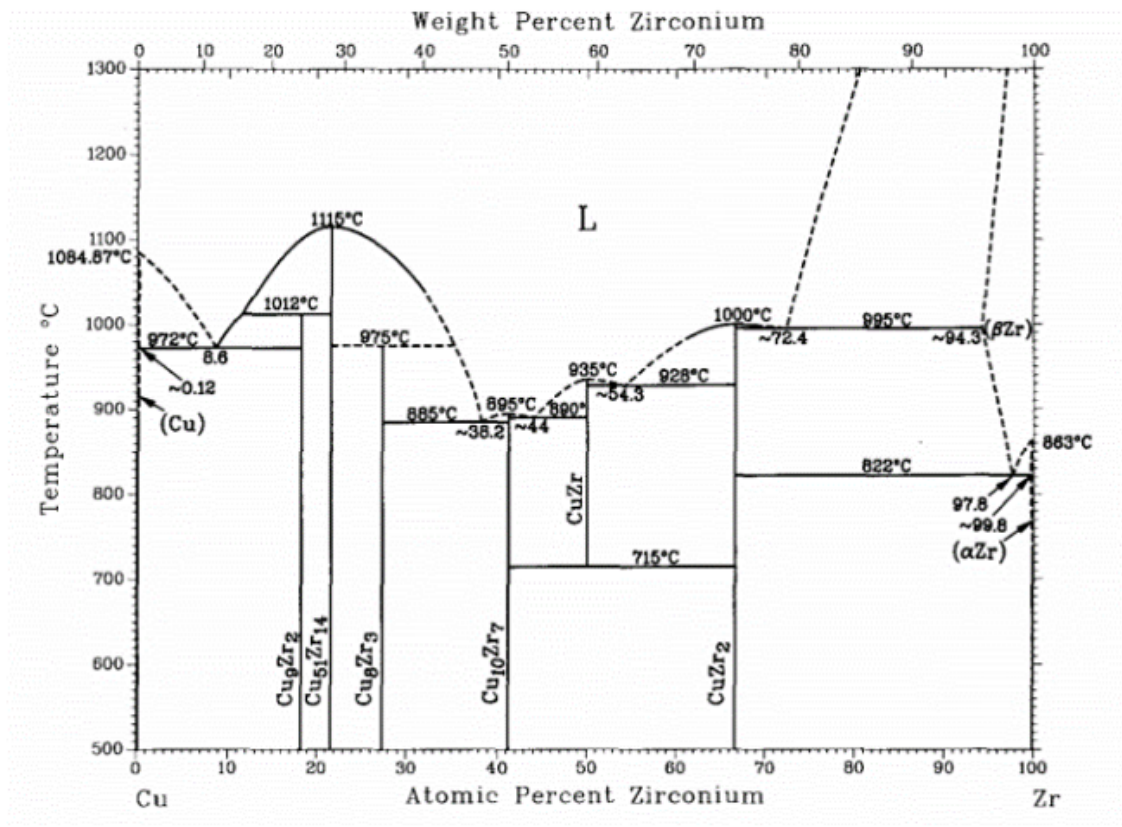Fig. 8. Simulated XRD pattern

27

Fig. 9. Experimental XRD [5]

Fig. 10. Copper-Zirconium Phase Diagram [15]

## 4.2 Glancing Angle Deposition

When atoms are deposited at oblique angles, shadowing effects occur. The line of sight for incoming atoms directed at the substrate is blocked by deposited atoms. Localized islands nucleate on the substrate that eventually form into rods. In figure 11 we modeled an experimental technique known as glancing angle deposition, for this technique we expect to see nanorods develop at oblique angles (approximately 85 degrees). The deposition angle of a binary system of atoms was varied between 45,60,and 85 degrees with respect to the normal of the substrate. At a deposition angle of 45 degrees we barely begin to see any shadowing effects occur. Some interfacial roughness is created by at this angle but nanorods have not started to form. At a deposition angle of 60 degrees we begin to see a little more clearly the shadowing effect. Nanorods are beginning to form but still are not clearly defined as there is little spacing if any between each nanorod. At an angle of 85 degrees the shadowing effect is very prominent and nanorods have very distinctly formed. Although the simulation box size is finite we can see that these effects are periodic in the x and y directions.
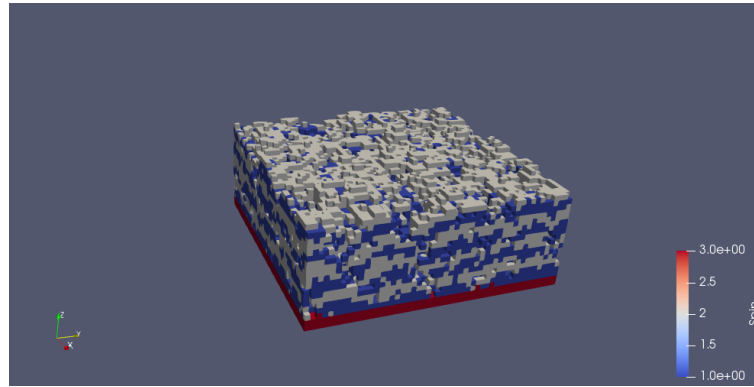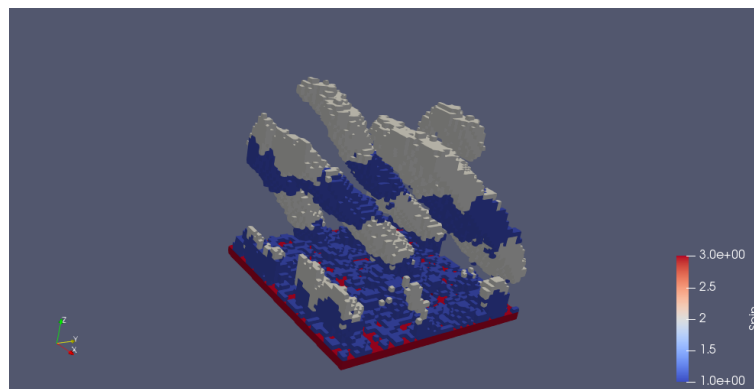
(a)
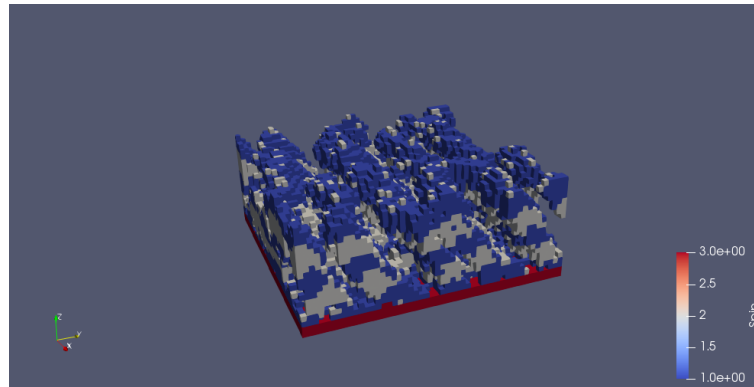


(b)



(c)

Fig. 11. The angle of the deposition flux was varied between 45 and 85 degrees. a) 45 degrees , b) 60 degrees, c) 85 degrees

## 4.3   Grain Formation
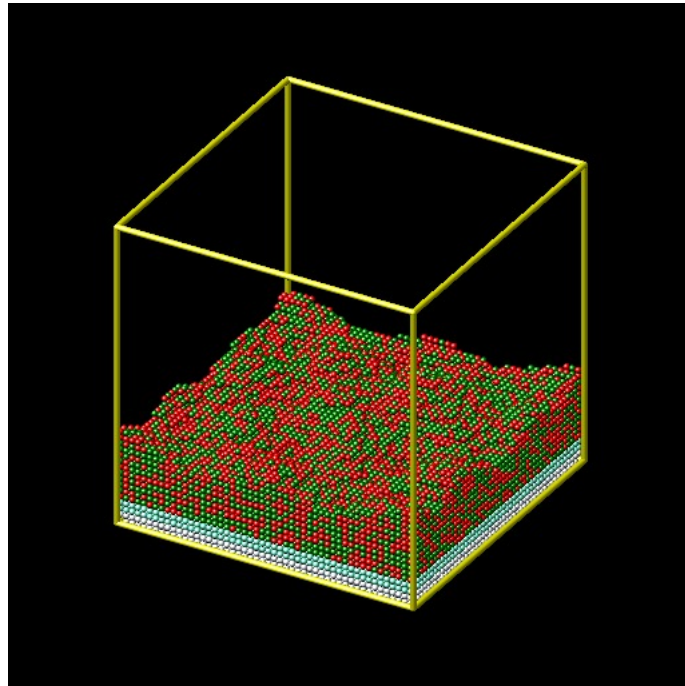


Fig. 12. Diffusion barrier dependent on atom type

We would like to create a model that allows us to notice the effects of diffusivity on the segregation of atomic species. This segregation is the cause of grain boundary formations. Figure 12 shows the results of a kMC simulation where the barrier of diffusion was dependent on the atom diffusing. Insteading of defining energy values for a site based off coordination number the diffusivity now only depends on the atom diffusing and not the neighbors around it. We can see that this does not produce much segregation and is not the primary factor in grain formation. To achieve grain formation the barrier has to have some dependency from the type of neighbor atoms surrounding that site. To achieve this we use an effective barrier instead. This effective barrier is a weighted average of the barriers a diffusing atom would have in a bulk crystal of each element. For example if an occupied site had one half of its

32

coordinated neighbor atoms of element A and another one half of element B then the effective barrier would be a half of barrier A and a half of barrier B. In figure 13 we see the result of co-depositing two atoms for a million timesteps. We choose energy barriers that make the elements chemically inert with each other to promote maximum grain formation. As we can see, the crystals grow separately and there is little contact between each type of atom as long as there is space for them to grow apart. This is of course not a physically realizable system because there will always be some kind of interaction between elements, however we show this here to make sure that our modifications to the program are functioning as we would expect. In
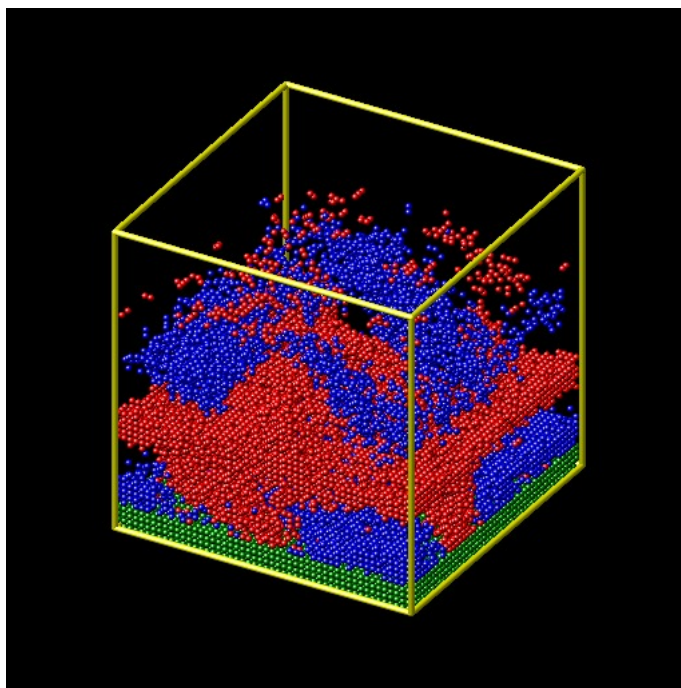


Fig. 13. Two elements that are chemically inert with each other through the selection of their energy barrier

figure 14 we explore different ratios of effective barriers. We can see that this has an effect on the grain formation and that for higher contrast in the effective barrier there is more segregation.
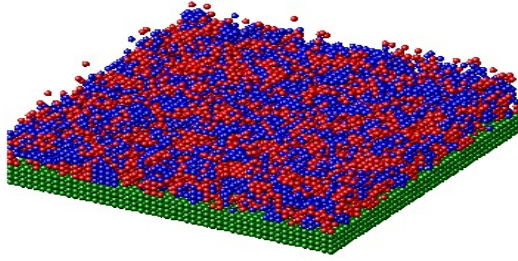
(a)
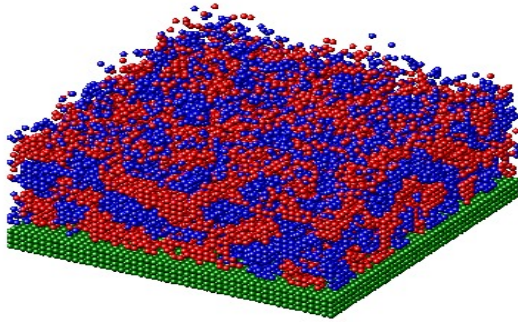


(b)

Fig. 14. These simulations use the effective barrier scheme. For figure a,there is a 2:1 ratio for the effective barrier. For figure b, there is a 10:1 ratio for the effective barrier.

Lastly, we simulate the growth of binary nanorods that exhibit grain formation in figure 15. A cross sectional view has been produced so that the morphology can

34

be more closely observed. The nano rods that we have simulated are deposited with a deposition angle of 85 degrees and a diffusion rate of 10:1. This produces nano rods that are at an angle of 44 degrees normal to the substrate. If we wanted to grow nano rods along only the (001) direction we could achieve this by rotating the deposition flux. The average grains produced by this method are approximately 3-4 atoms thick. The thickness of the grains and nanorods can be altered by adjusting the deposition rate and the time for the simulation. These two variables can have dramatic results on the simulation because they control how much diffusion occurs. If the deposition rate is too high then deposited atoms do not have a chance to diffuse along the surface and minimize their energy before other atoms deposit on top of them. If the simulation time is too short then the atoms are simply not given a chance to diffuse. Increasing the simulation time can ensure proper sampling but will also increase the computational time.
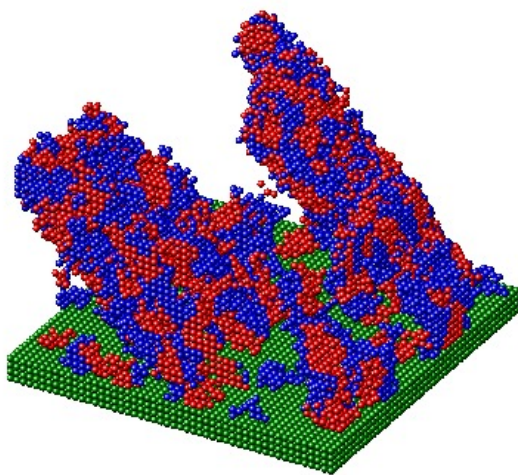
(a) Grain formations within nanorods



(b) Cut out of nanorods

36

Fig. 15. Glancing angle deposition of binary alloys with significant atom segregation
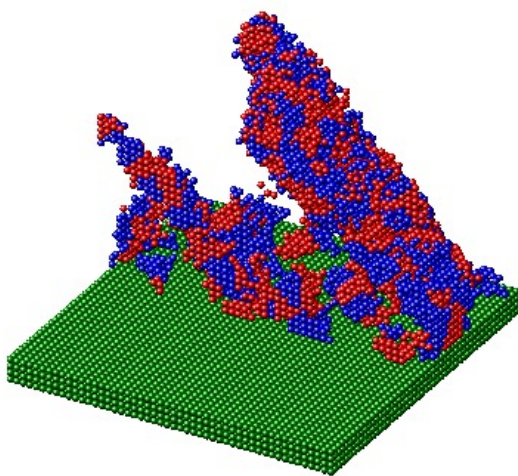
# CHAPTER 5

## CONCLUSION AND FUTURE WORK

This study has shown how the fast simulation of dynamics via the kMC method can be combined with a MD type approach to gain insights about binary alloys. The reduction of time saved by using the kMC approach over the MD approach to simulate the dynamics allowed us to create simulation sizes large enough to view the features of a deposited film using only a single processor instead of having to run simulations in parallel.Overall the time it took for a simulation run reduced from days to hours when using Monte Carlo methods over molecular dynamics to simulate deposition.

Our simulations showed that vast amount of morphologies can be created based off of factors as simple as the deposition angle and energy barriers. MD was used to relax the crystal structure and add physical meaning. We verified our results experimentally by calculating a theoretical X-Ray diffraction pattern and compared the result to known patterns in the literature. We found that the peaks relative to each other were in good correspondence with the experimental values, however peak shapes were broadened. We were also able to identify the parameters that promote grain formation and simulate this phenomenon in nanorods.

In the future, it would be advantageous to obtain a better determination of the diffusion barriers for each element. We did not use MD to determine any specific energy barriers here because we wanted the study to remain focused on kMC techniques over MD as MD has plenty of documentation in the literature. At room temperature the energy defintions of our copper-zirconium system are of little consequence because of the lack of aggregation and the use of MD after our kMC simulation. At higher

temperatures required to simulate fast cooling of metallic glasses this error could play a more prominent role [16]. When looking at the phase diagram for the copper-zirconium system presented earlier in this study we see that at temperatures roughly 1000 degrees celsius there are a lot of critical transformations that could occur which would require a higher degree of simulation accuracy. These phase transformations would also require a different method of importance sampling since the probabilty distribution does not retain its ergodicity.

# Appendix A

## ABBREVIATIONS

VCU           Virginia Commonwealth University

RVA           Richmond Virginia

PVD           Physical Vapor Deposition

kMC           kinetic Monte Carlo

MC           Monte Carlo

MD           Molecular Dynamics

MG           Metallic Glasss

XRD           X-Ray Diffraction

GLAD           Glancing Angle Deposition

SPPARKS    Stochastic Parallel PARticle Kinetic Simulator

LAMMPS    Large-scale Atomic/Molecular Massively Parallel
Simulator

# Appendix B

## SCRIPTS AND C/C++ CODE

The code that ran the simulations in this thesis has been posted to Github under the username marshalltc. SPPARKS and LAMMPS are both written in C/C++ where the syntax is mostly C but the higher level elements of programming implented in C++. The modifications to SPPARKS code is available on Github as well as scripts that were ran.

## EXCERPT OF C/C++ CODE

```
622        lattice[i] = VACANT;
623        lattice[j] = OCCUPIED;
624
625        // efinal = i,j and their neighbors
626        // use pcheck[] to avoid recomputing energy of same site
627
628        efinal = site_energy(i) + site_energy(j);
629        nsites = 0;
630        psites[nsites++] = i;
631        psites[nsites++] = j;
632        pcheck[i] = pcheck[j] = 1;
633
634        for (k = 0; k < numneigh[i]; k++) {
635          m = neighbor[i][k];
636          if (pcheck[m]) continue;
637          efinal += site_energy(m);
638          psites[nsites++] = m;
639          pcheck[m] = 1;
640        }
641        for (k = 0; k < numneigh[j]; k++) {
642          m = neighbor[j][k];
643          if (pcheck[m]) continue;
644          efinal += site_energy(m);
645          psites[nsites++] = m;
646          pcheck[m] = 1;
647        }
648
649        for (m = 0; m < nsites; m++) pcheck[psites[m]] = 0;
650
651        edelta = efinal - einitial;
652
653        if (!barrierflag) {
654          if (edelta <= 0.0) probone = 1.0;
655          else if (temperature > 0.0)
656        probone = exp(-edelta*t_inverse);
657        }
658
659      else if (temperature > 0.0){
660   //marshalltc
661        int num_types = 3;//sizeof(barrier)/sizeof(barrier[0]);
662        double ntotal = 0;
663        //double ntype[num_types];
664        double ntype[3] = {0,0,0};
665        double percent_atom[num_types];
666        double barrier_eff = 0;
667        int site_type = iarray[1][i] - 1;
668
669        for (int j = 0; j < numneigh[i]; j++){
670            for(int k = 0; k < num_types; k++){
671              if (iarray[1][neighbor[i][j]] == k + 1) ntype[k]++;
672            }
673        }
674
675        for(int k = 0; k < num_types; k++) ntotal += ntype[k];
676        for(int k = 0; k < num_types; k++) percent_atom[k] = ntype[k]/ntotal;
677        for(int k = 0; k < num_types; k++) barrier_eff +=
678        percent_atom[k]*barrier[site_type][k];
679
680
681              if (edelta <= 0.0)
682              probone = exp(-barrier_eff * t_inverse);
683              else
684              probone = exp((-edelta - barrier_eff) * t_inverse);
685      }
686   //end of my code
687
688
689        if (probone > 0.0) {
```

Fig. 16. Section of C/C++ code containing propensity calculation

# Appendix D

## SPPARKS SCRIPT

```
1    seed 56689
2    app_style diffusion nonlinear hop
3    dimension 3
4    lattice sc/26n 1
5    region myregion block 0 50 0 50 0 50
6    create_box myregion
7    create_sites box
8    set site value 1
9    set site value 2 if z < 4.0
10   set site value 3 if z < 2.0
11   set site value 3 if z > 49.0
12
13
14   barrier hop 1 .01 .02 .03
15   barrier hop 2 .1 .2 .3
16   barrier hop 3 1000 1000 1000
17
18   temperature .0257
19   solve_style linear
20
21   dump imagedump image 100 data/image*.ppm i2 i1 crange 0 10 sdiam 1
22   dump_modify imagedump thresh i1 > 1
23   dump_modify imagedump scolor 1 red
24   dump_modify imagedump scolor 2 blue
25   dump_modify imagedump scolor 0 green
26   dump_modify imagedump pad 6
27
28   variable i loop 1000
29   label loop
30    deposition .1 0 0 -1 1.0 9 26 2
31    run 10
32    deposition .1 0 0 -1 1.0 9 26 1
33    run 10
34   next i
35   jump in.spparks loop
36
37
```

Fig. 17. An example of a SPPARKS script to model binary alloys

# BIBLIOGRAPHY

[1] Szab, B., Szabo, B. A., Babuka, I. (1991). Finite element analysis. John Wiley Sons.

[2] Yang, W., Ayers, P. W. (2003). Density-functional theory. In Computational Medicinal Chemistry for Drug Discovery (pp. 103-132). CRC Press.

[3] Voter A.F. (2007) INTRODUCTION TO THE KINETIC MONTE CARLO METHOD. In: Sickafus K.E., Kotomin E.A., Uberuaga B.P. (eds) Radiation Effects in Solids. NATO Science Series, vol 235. Springer, Dordrecht

[4] Hawkeye, M. M., Taschuk, M. T. and Brett, M. J. (2014). Introduction: Glancing Angle Deposition Technology. In Glancing Angle Deposition of Thin Films (eds M. M. Hawkeye, M. T. Taschuk and M. J. Brett). doi:10.1002/9781118847510.ch1

[5] Lu Xie, Pascal Brault, Anne-Lise Thomann, Larbi Bedra. Molecular dynamic simulation of binary ZrxCu100-x metallic glass thin film growth. Applied Surface Science, Elsevier, 2013, 274, pp.164 -170. ¡hal-00797237¿

[6] Julian Goldsmid, H. (2014). Bismuth Telluride and Its Alloys as Materials for Thermoelectric Generation. Materials. 7. 10.3390/ma7042577.

[7] Landau, D., Binder, K. (2005). A guide to Monte Carlo simulations in statistical physics (2nd ed.). Cambridge ; New York: Cambridge University Press.

[8] Chatterjee, A., Vlachos, D. G. (2007). An overview of spatial microscopic and accelerated kinetic Monte Carlo methods. Journal of computer-aided materials design, 14(2), 253-308.

[9] Crossing the Mesoscale No-Man's Land via Parallel Kinetic Monte Carlo, S. Plimpton, C. Battaile, M. Chandross, L. Holm, A. Thompson, V. Tikare, G. Wagner, E. Webb, X. Zhou, C. Garcia Cardona, A. Slepoy, Sandia report SAND2009-6226,

October 2009

[10] Sherlock, C., Fearnhead, P., Roberts, G. O. (2010). The random walk Metropolis: linking theory and practice through a case study. Statistical Science, 25(2), 172-190.

[11] Allen, M. P., Tildesley, D. J. Molecular Dynamics Simulations.

[12] S. Plimpton, Fast Parallel Algorithms for Short-Range Molecular Dynamics, J Comp Phys, 117, 1-19 (1995)

[13] Dodson, B. W. (1987). Development of a many-body Tersoff-type potential for silicon. Physical Review B, 35(6), 2795.

[14] S. P. Coleman, D. E. Spearot, L. Capolungo, MSMSE, 21, 055020 (2013)

[15] Arias, D., Abriata, J. P. (1990). Cu-Zr (copper-zirconium). Journal of Phase Equilibria, 11(5), 452-459.

[16] Kumar, G., Desai, A., Schroers, J. (2011). Bulk metallic glass: the smaller the better. Advanced materials, 23(4), 461-476.